

The Size-Power Tradeoff in HAR Inference: Supplement

August 1, 2019

Eben Lazarus
MIT Sloan

Daniel J. Lewis
Federal Reserve Bank of NY

James H. Stock
Harvard University

This supplement provides additional figures and Monte Carlo results.

Figure S.1 plots the implied mean kernel for the Fourier, cosine, and SS basis functions for $B = 8$ and $T = 200$. The Fourier transforms of these implied mean kernels, that is, the frequency-domain implied mean kernel, are plotted in Figure S.2 at the frequencies $2\pi j/T, j = 0, \dots, 35$. The EWP (Fourier) estimator is the only one of these four that has an exact kernel representation, and its frequency-domain kernel is the familiar flat (Daniell) kernel that gives equal weight to the first $B/2$ periodogram ordinates. The remaining three implied mean kernels in the frequency domain also concentrate their mass at low frequencies.

Figure S.3 shows the power difference, as a function of the local alternative index δ , between the EWP and QS test, for $B = 8$ for EWP and b for QS chosen so that the two tests have the same size. This curve is computed using the expression in Theorem 3 and Remark 6.

Figure S.4 shows additional Monte Carlo results for different values of T for 6 tests: QS, EWP, cosine (type II cosine basis function), NW, and SS.

Figure S.5 shows the spectral density for the ARMA(2,1) process. The parameters are calibrated so that $\omega^{(2)} = 4$ (the same as an AR(1) with $\rho = 0.5$) and with a spectral density approximately symmetric around $\pi/2$, with a minimum at $\pi/2$ (the coefficients are $\rho_1 = 0.048, \rho_2 = 0.248, \theta = -0.064$).

Figure S.6 shows results for ARMA(2,1) disturbances, $m = 1$.

Figures S.7 and S.8 show additional results for $m = 2$.

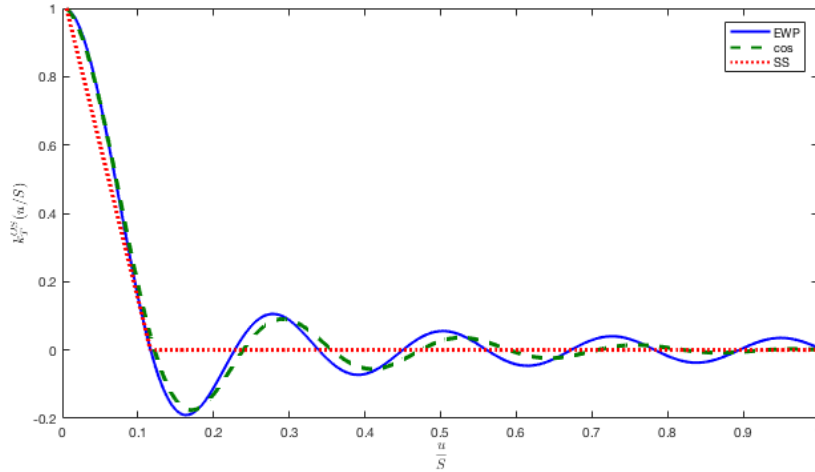


Figure S.1. Implied mean kernel of basis function estimators with $B = 8$, time domain: Fourier/EWP (blue, solid), cosine (green, dash), and split-sample (red, dot).

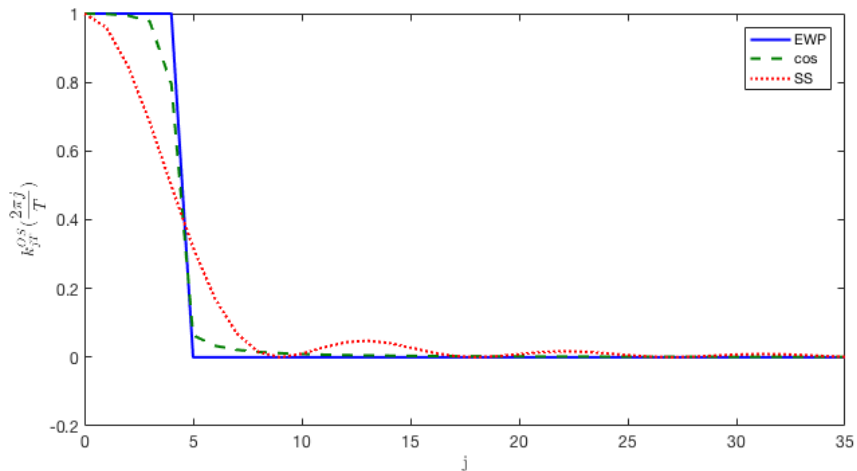


Figure S.2. Implied mean kernel of basis function estimators with $B = 8$, frequency domain: Fourier/EWP (blue, solid), cosine (green, dash), and split-sample (red, dot). The frequency domain kernel is normalized to 1 at $\omega = 0$ and computed over the periodogram ordinates (so the horizontal axis value j corresponds to $2\pi j/T$, etc.).

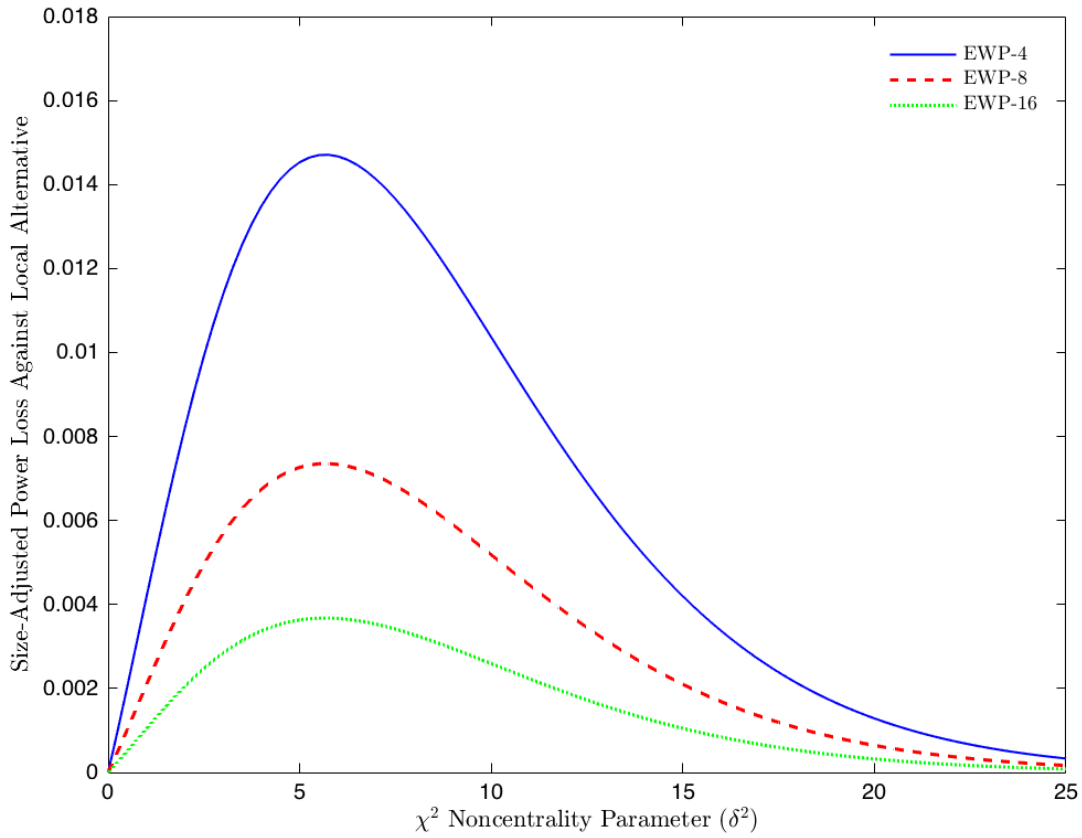


Figure S.3. Small- b approximation to power loss for EWP test, compared to QS test, for different values of B in the EWP test and with b for the QS test chosen so that the EWP and QS tests have the same higher-order size when evaluated using fixed- b critical values. The figure plots the final expression in (44) as a function of δ . Gaussian location model, $m=1$, 5% significance level.

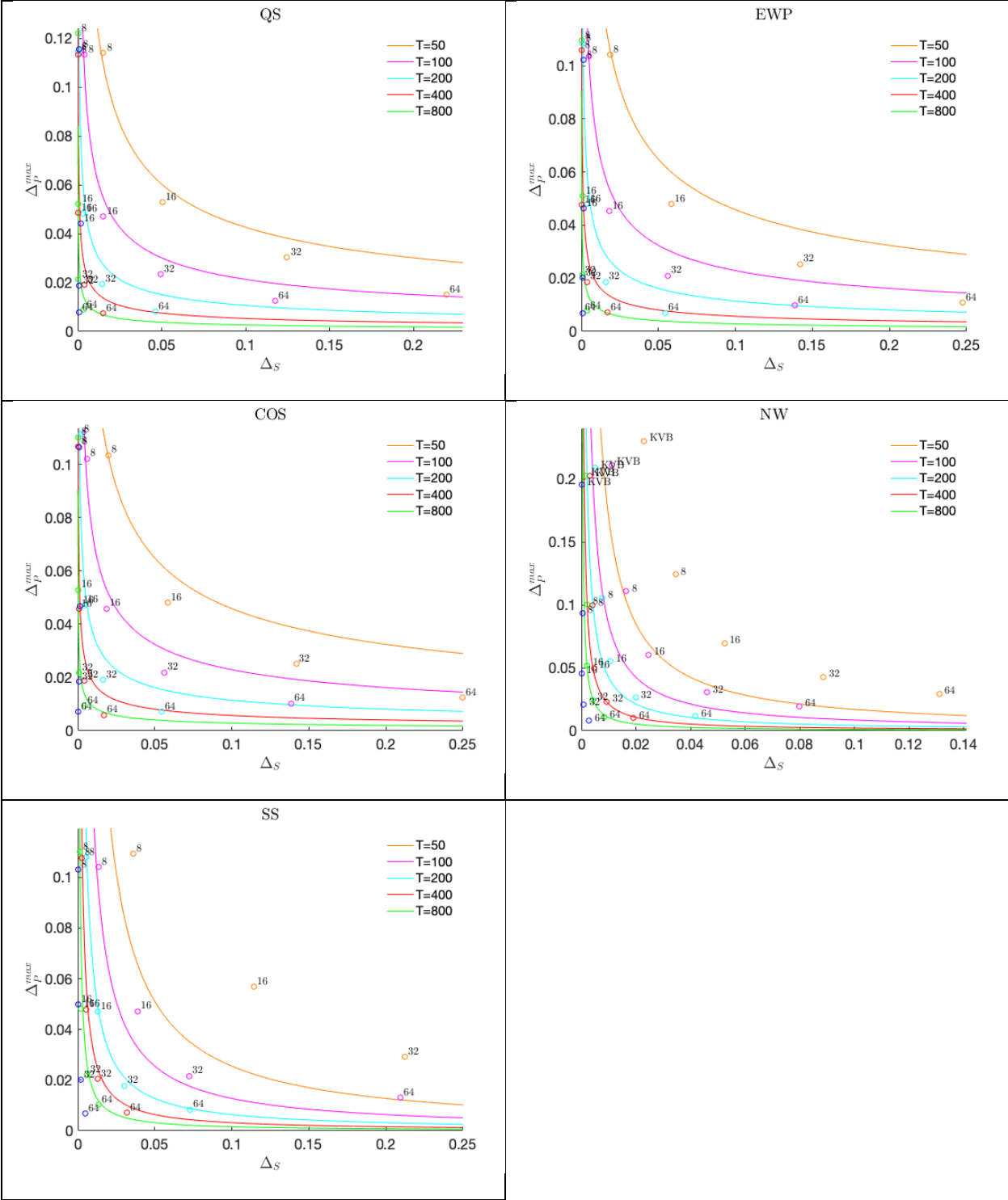


Figure S.4. Location model, AR(1), $m = 1, \rho = 0.5$.
 Theoretical size distortion/power loss trade-off curves for each estimator with Monte Carlo results for T ranging from 50 to 1600.

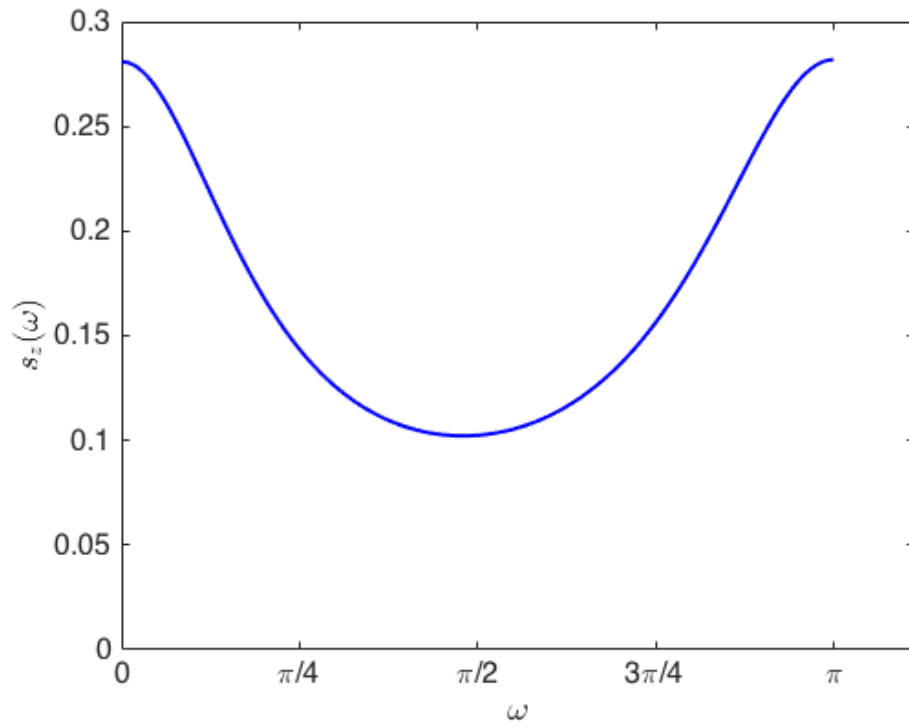


Figure S.5. Spectral density of calibrated ARMA(2,1), $\omega^{(2)} = 4$.

ARMA(2,1) Model

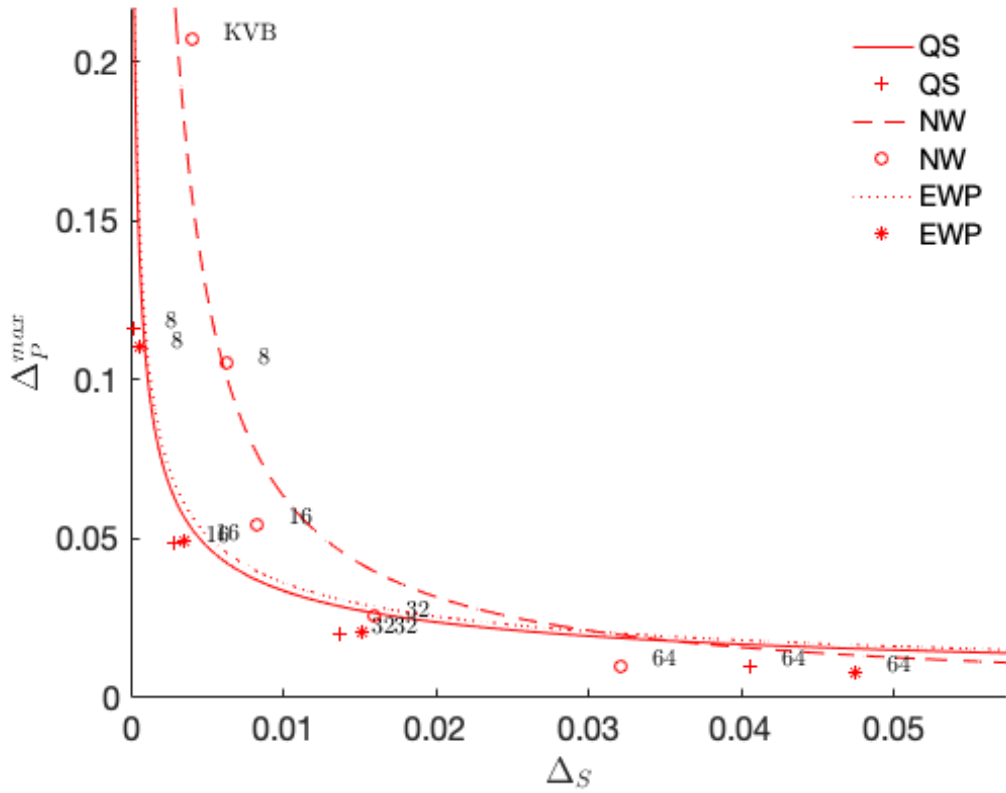


Figure S.6. Location model, ARMA(2,1), $m = 1$, $T = 200$.

Theoretical size distortion/power loss trade-off curves for QS, Newey-West, and EWP estimators with Monte Carlo results. ARMA(2,1) parameters fixed such that $\omega^{(2)} = 4$, equivalent to AR(1) with $\alpha = 0.5$ (parameter values as in Figure S.5).

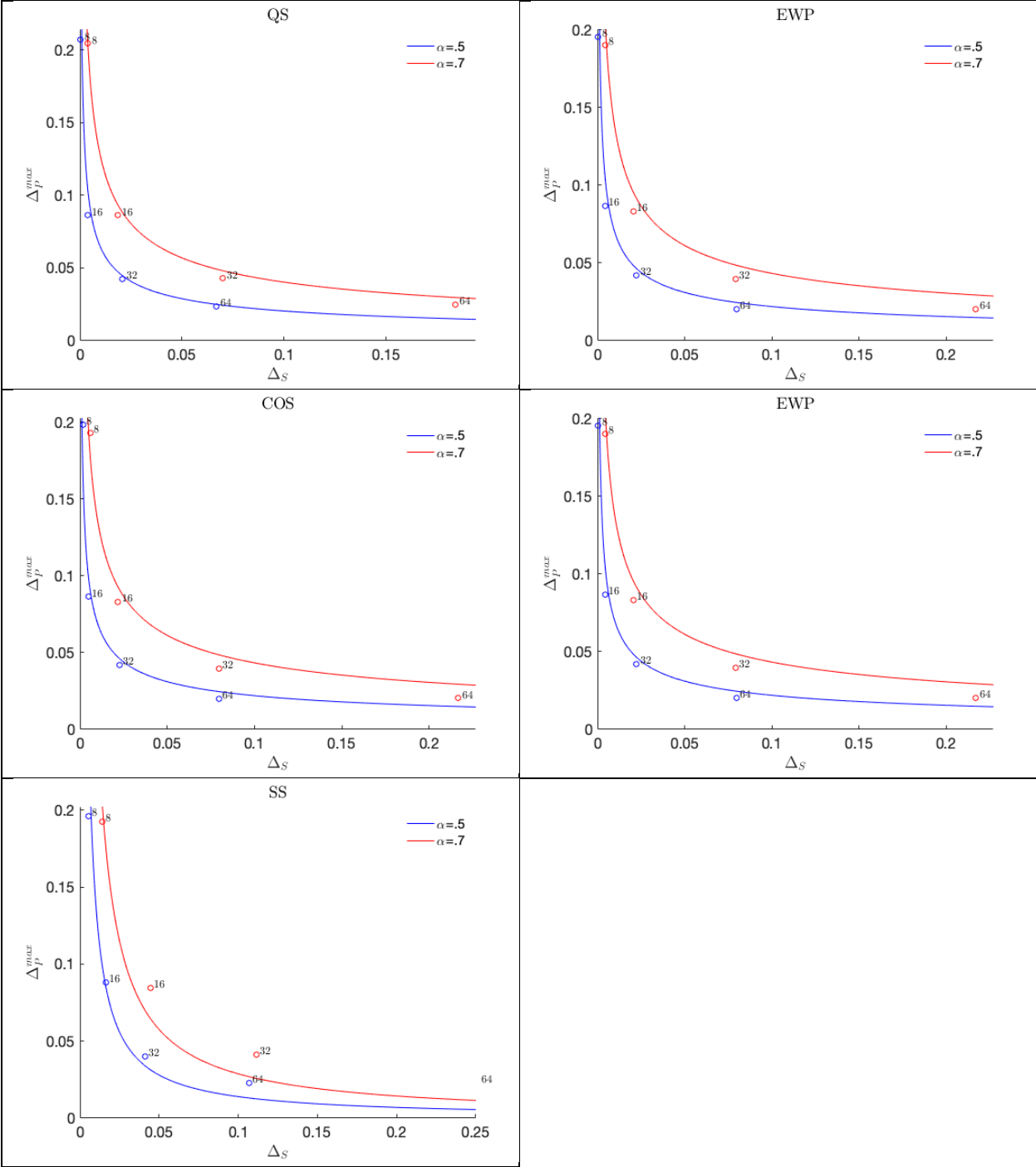


Figure S.7. Location model, AR(1), $m = 2$, $\rho = .5$ and $.7$, $T = 200$. Theoretical size distortion/power loss trade-off curves for each estimator and Monte Carlo results (dots).

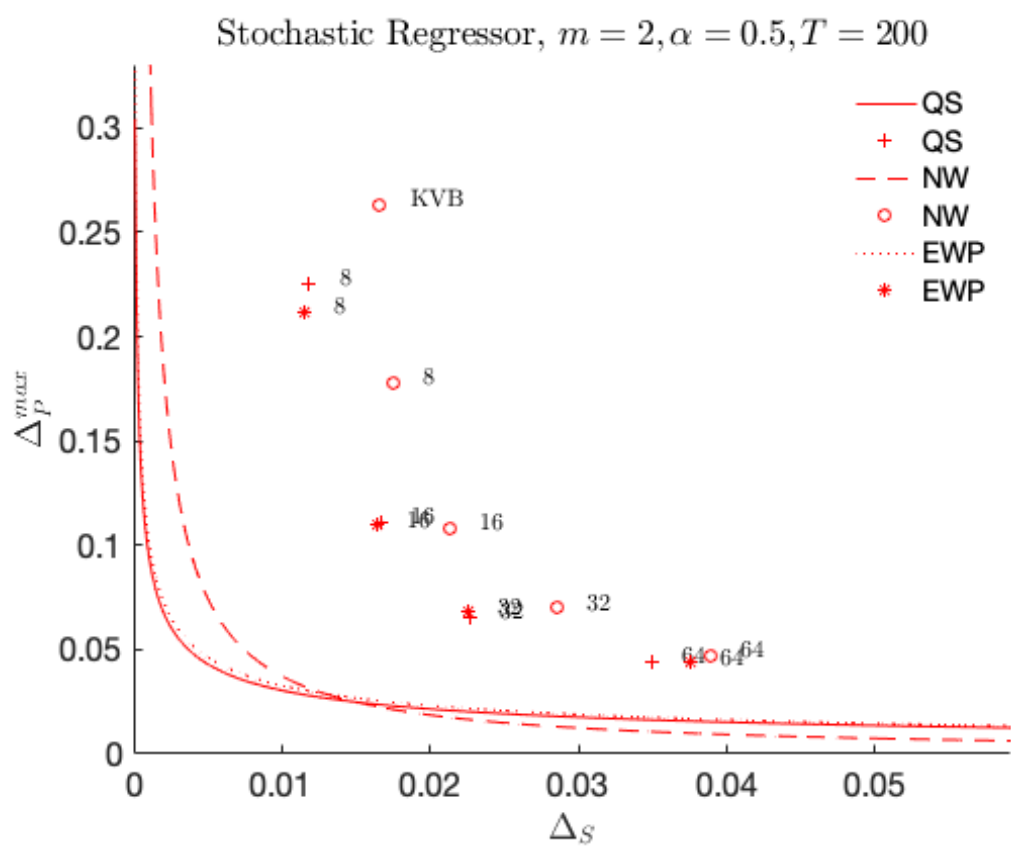


Figure S.8. Stochastic regressor, AR(1), $m = 2, \rho = 0.5, T = 200$. Theoretical size distortion/power loss trade-off curves for QS, Newey-West, and EWP estimators with Monte Carlo results. *Note:* Curves are for the Gaussian location model.